Broadband control of emission wavelength of InAs/GaAs quantum dots by GaAs capping temperature

Kaizu, Toshiyuki

Matsumura, Takuya

Kita, Takashi

(Citation)
Journal of Applied Physics,118(15):154301-154301

(Issue Date)
2015-10-21

(Resource Type)
journal article

(Version)
Version of Record

AIP | Journal of Applied Physics

Broadband control of emission wavelength of InAs/GaAs quantum dots by GaAs capping temperature

Toshiyuki Kaizu, Takuya Matsumura, and Takashi Kita

Citation: Journal of Applied Physics **118**, 154301 (2015); doi: 10.1063/1.4933182
View online: http://dx.doi.org/10.1063/1.4933182
View Table of Contents: http://scitation.aip.org/content/aip/journal/jap/118/15?ver=pdfcov
Published by the AIP Publishing

Broadband control of emission wavelength of InAs/GaAs quantum dots by GaAs capping temperature

Toshiyuki Kaizu,[1,2,a)] Takuya Matsumura,[2] and Takashi Kita[2]
[1]*Center for Supports to Research and Education Activities, Kobe University, 1-1 Rokkodai, Nada, Kobe 657-8501, Japan*
[2]*Department of Electrical and Electronic Engineering, Graduate School of Engineering, Kobe University, 1-1 Rokkodai, Nada, Kobe 657-8501, Japan*

(Received 15 June 2015; accepted 2 October 2015; published online 15 October 2015)

We investigated the effects of the GaAs capping temperature on the morphological and photoluminescence (PL) properties of InAs quantum dots (QDs) on GaAs(001). The broadband tuning of the emission wavelength from 1.1 to 1.3 μm was achieved at room temperature by only adjusting the GaAs capping temperature. As the capping temperature was decreased, the QD shrinkage due to In desorption and In-Ga intermixing during the capping process was suppressed. This led to QDs with a high aspect ratio, and resultantly, the emission wavelength shifted toward the longer-wavelength side. In addition, the linearly polarized PL intensity elucidated anisotropic characteristics reflecting the shape anisotropy of the embedded QDs, in which a marked change in polarization anisotropy occurred at capping temperatures lower than 460 °C. © *2015 AIP Publishing LLC*. [http://dx.doi.org/10.1063/1.4933182]

I. INTRODUCTION

Self-assembled InAs quantum dots (QDs) have attracted considerable attention because of their potential applications to advanced optical devices such as laser diodes with low threshold current density and high-temperature stability[1–3] and polarization-insensitive semiconductor optical amplifiers (SOAs).[4–9] These devices are required to operate not only in the optical communication wavelength bands of 1.3 and 1.55 μm but also in the shorter bands of 1.0–1.3 μm expected to be used in the future expansion of optical networking. In particular, SOAs operating in the wavelength region of 1.0–1.3 μm are essential because of the large attenuation of silica glass optical fibers.[10] We have recently fabricated QD-SOA device structures containing 30 and 40 layers of closely stacked InAs/GaAs QDs, and demonstrated the polarization-insensitive properties of the net modal gain in the wavelength region of 1.1–1.2 μm using the Hakki-Paoli method.[9] To achieve a broader operational bandwidth, control of the QD energy levels is important. The energy levels and corresponding emission wavelengths of QDs are significantly affected by the variation in QD size during the GaAs capping process as well as that in as-grown QD size, which varies with the QD growth conditions. GaAs capping induces In desorption from the InAs QD surfaces and the intermixing of In and Ga atoms at the interface between the QDs and the cap layer owing to the compressive lattice strain,[11,12] which results in QD shrinkage and a shift of the emission wavelength toward the shorter-wavelength side.[13] The introduction of an InGaAs strain-reducing layer (SRL)[14,15] and an In flushing process[16,17] enables the emission wavelength of InAs QDs to be controlled by adjusting the variation in QD size during the capping process. These methods, however, have disadvantages when fabricating the multiple-stacked QD structures used as device active layers, such as the generation of stacking faults due to the accumulation of lattice strain in the entire structure used for the SRL and the complex sequence of substrate temperatures required for In flushing.

In this study, we investigated the control of the photoluminescence (PL) emission wavelength of InAs QDs by the substrate temperature during the conventional GaAs capping process. A decrease (increase) in the GaAs capping temperature suppressed (enhanced) In desorption and In-Ga intermixing, and thereby, the broadband shift of the emission wavelength from 1.1 to 1.3 μm was achieved at room temperature. In addition, we revealed the variations in PL polarization properties caused by the QD shape anisotropy after capping.

II. EXPERIMENTAL PROCEDURE

The samples were grown on semi-insulating GaAs(001) substrates by solid-source molecular beam epitaxy. The substrate temperatures were monitored using an infrared pyrometer. After the removal of an oxide layer at 585 °C, a 400-nm-thick GaAs buffer layer was deposited at 550 °C. Then, the substrate temperature was lowered to 480 °C. A c(4 × 4) reconstructed surface was confirmed by reflection high-energy electron diffraction (RHEED). InAs QDs with a nominal thickness of 2.0 monolayers (ML) were grown by self-assembly, and then, the growth was interrupted for 60 s, during which the substrate temperature was varied between 430 and 495 °C. Subsequently, a 100-nm-thick GaAs cap layer was deposited. The growth rates of InAs and GaAs were 0.04 and 0.8 ML s^{-1}, respectively, and the As_2 beam equivalent pressure (BEP) was 1.3×10^{-3} Pa. The arrival rate of As_2 species which can be derived from the BEP and GaAs growth rate,[18] was 8.7×10^{15} cm^{-2} s^{-1}, and the adsorption rate of As atoms to GaAs lattice sites was

a)Electronic mail: kaizu@crystal.kobe-u.ac.jp

$5.0 \times 10^{14}\,\mathrm{cm}^{-2}\cdot\mathrm{s}^{-1}$. The evolution of the surface morphology during the InAs QD growth and GaAs capping was monitored by the RHEED. The QD morphology after capping was analyzed by cross-sectional high-angle annular dark-field scanning transmission electron microscopy (HAADF-STEM). PL and polarized PL measurements were performed using a continuous-wave laser diode with a wavelength of 659 nm. The PL signal was dispersed using a 30 cm single monochromator and detected using a liquid-nitrogen-cooled InGaAs diode array. In addition, time-resolved PL measurements were performed using a near-infrared streak camera system with a temporal resolution of 20 ps. The light source used was a mode-locked Ti:sapphire pulse laser with a pulse width of 130 fs and a repetition rate of 80 MHz. The excitation wavelength and excitation power density were 800 nm and 0.06 $\mathrm{nJ/cm}^2$, respectively.

III. RESULTS AND DISCUSSION

The RHEED patterns obtained during the initial growth of the GaAs cap layer are shown in Figs. 1(a) and 1(b). As the growth of the cap layer proceeds, the RHEED pattern changes from spots [Fig. 1(a)] originating from three-dimensional islands to streaks. The reconstructed surface was a single phase of (2×4) at capping temperatures higher than 470 °C, while at capping temperatures lower than 470 °C, it was a mixture of c(4×4) and (2×4) phases [Fig. 1(b)]. The streak patterns indicate that the InAs QDs are completely embedded in the cap layer, resulting in the formation of a two-dimensional surface. Correspondingly, the diffraction spot intensity gradually decreases with an increasing cap layer thickness and then saturates, as shown in Fig. 1(c). The cap layer thickness θ at which the QDs were embedded was estimated from the variation in the RHEED intensity in Fig. 1(c) and is plotted as a function of the capping temperature in Fig. 1(d). As the capping temperature is decreased, the value of θ monotonically increases. This suggests the suppression of QD shrinkage due to In desorption and In-Ga intermixing during the initial growth of the cap layer.

To analyze the InAs QD size after GaAs capping in detail, the cross-sectional observations of the morphology of QDs embedded with the cap layer were performed by HAADF-STEM. Figure 2(a) shows the high-resolution (110) cross-sectional HAADF-STEM images of InAs QDs embedded with three different capping temperatures, in which the morphology of the QDs on the InAs wetting layer with a thickness about 2 ML can be clearly observed. We selected the largest QD from more than 10 cleaved-QDs for each capping temperature and derived the base size and height, which is a reliable method to obtain information of a QD cleaved near the center. We derived the aspect ratios averaging the values of more than 10 cleaved-QDs because it almost did not depend on the cleavage positions. The results are summarized in Figs. 2(b) and 2(c). Compared with the height of the as-grown QDs derived by atomic force microscopy (AFM), the height of the embedded QDs decreases at all capping temperatures. However, the reduction of height becomes smaller with decreasing capping temperature. This

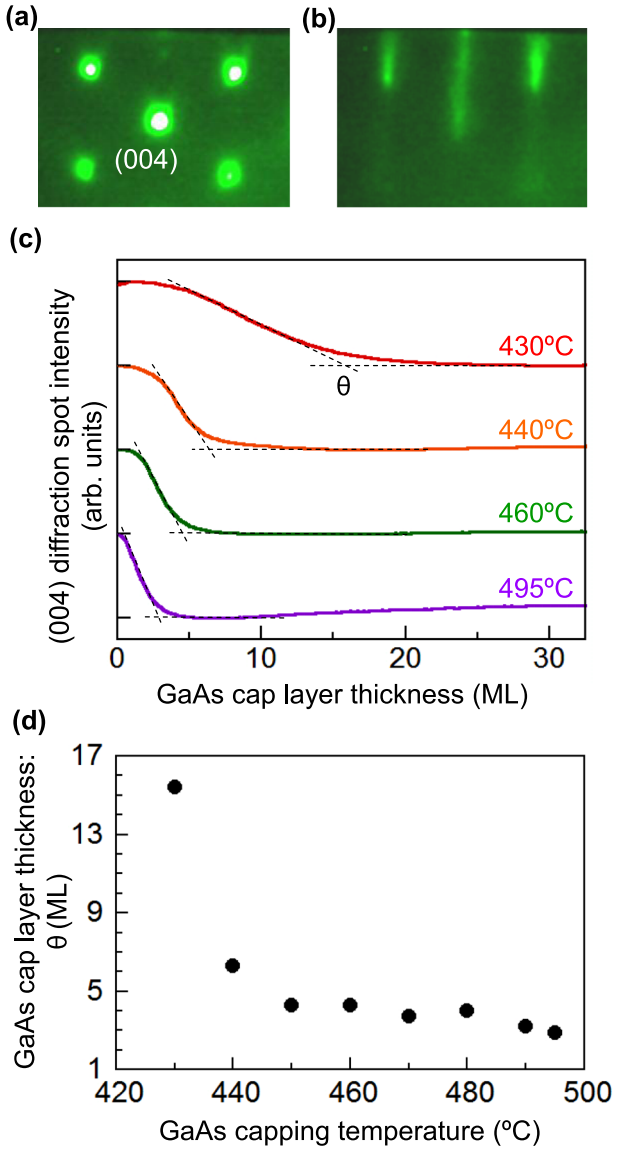

FIG. 1. RHEED patterns of the (a) InAs QD surface and (b) 24-ML-thick GaAs cap layer surface along the [−110] azimuth. (c) (004) diffraction spot intensity as a function of the GaAs cap layer thickness for various capping temperatures. (d) GaAs capping temperature dependence of θ, where θ is the GaAs cap layer thickness at which the InAs QDs were embedded.

agrees with the RHEED results, which indicate the suppression of QD shrinkage. The [−110] base size increases up to the capping temperature of 460 °C, below which it becomes almost constant. It follows that the aspect ratio of the QDs after capping depends on the capping temperature, as shown in Fig. 2(c).

These morphological variations in the QDs during the capping process significantly affect the optical properties of the QDs. Figure 3(a) shows the room-temperature PL spectra of the InAs QDs, and Fig. 3(b) shows the PL peak wavelength and full width at half maximum (FWHM) as functions of the GaAs capping temperature. All the PL spectra have a shoulder on the shorter-wavelength side on the main peak, which originates from the excited-state transition of the QDs. The peak wavelength is monotonically shifted toward the longer-wavelength side with decreasing capping temperature, and thereby, broadband tuning from 1.1 to 1.3 μm is

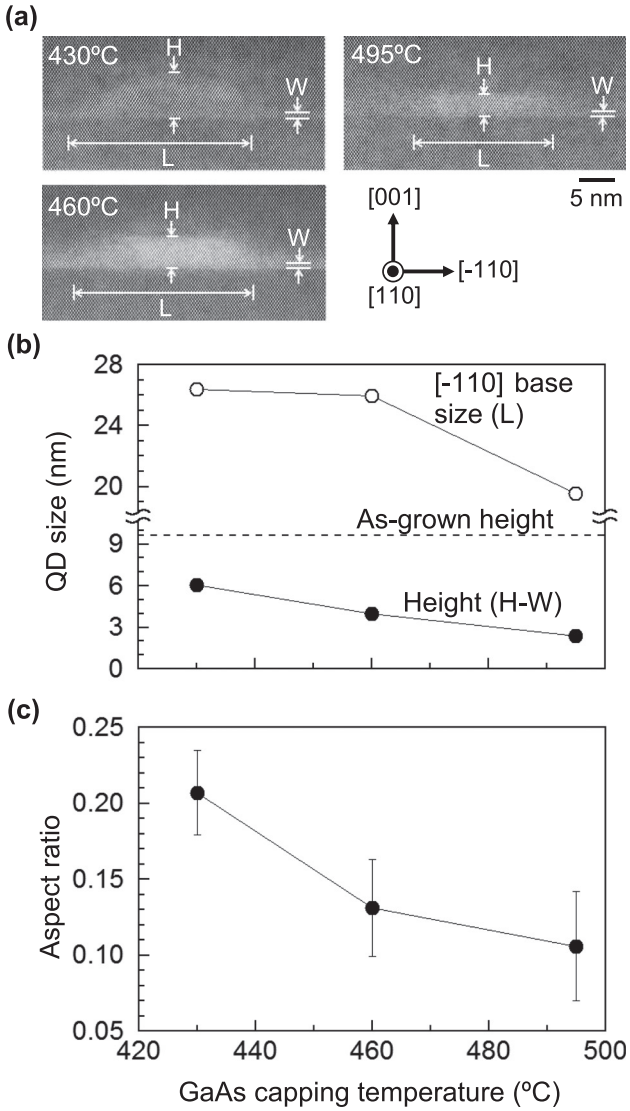

FIG. 2. (a) High-resolution (110) cross-sectional HAADF-STEM images of the InAs QDs embedded with GaAs capping temperatures of 430, 460, and 495 °C. (b) [−110] base size (L, open symbols) and height (H-W, filled symbols) as a function of the GaAs capping temperature. This was derived by analyzing the largest QD among more than 10 cleaved-QDs for each capping temperature. The dotted line represents the height of the as-grown QDs derived from AFM observations. (c) Aspect ratio of the InAs QDs after capping as a function of the GaAs capping temperature. This was derived by averaging the values of more than 10 cleaved-QDs for each capping temperature. The symbols and error bars represent the average values and standard deviations, respectively.

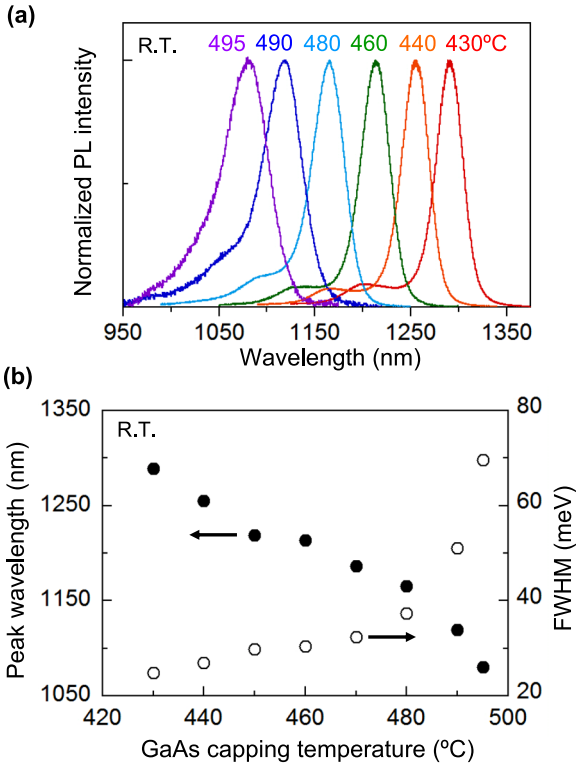

FIG. 3. (a) Room-temperature PL spectra of the InAs QDs and (b) PL peak wavelength (filled symbols) and FWHM (open symbols) as functions of the GaAs capping temperature.

achieved at room temperature. This shift is larger than that reported in a previous study using an As_4 source.[19] The PL FWHM markedly decreases with decreasing the capping temperature. When the capping temperature becomes lower than 470 °C, the FWHM exhibits almost constant value. To explain this behavior, we investigated the measurement temperature dependence of the PL peak energy. The results for various capping temperatures are shown in Fig. 4(a). The solid lines represent the energy gap shrinkage of the QDs estimated from the Varshni empirical relation[20]

$$E(T) = E(0) - \frac{\alpha T^2}{\beta + T}, \quad (1)$$

where $E(0)$ is the energy gap at 0 K and α and β are the Varshni coefficients. The parameters determined by fitting to the measured data in the low temperature region below 120 K and the high temperature region above 220 K are listed in Table I. The PL peak energy exhibits a sigmoidal dependence on the measurement temperature, which is interpreted as the thermally induced transfer of carriers from smaller to larger QDs.[21,22] This feature of the bimodal distribution of the QD size becomes pronounced with increasing capping temperature. Therefore, the energy difference between the $E(0)$ of the smaller QDs and that of the larger QDs, $\Delta E(0)$, increases, as shown in Fig. 4(b). It is noted that $\Delta E(0)$ is smaller than the energy difference between the ground- and excited-states of the QDs. The capping temperature dependence of $\Delta E(0)$ corresponds well with that of the PL FWHM in Fig. 3(b), from which the dispersion of the bimodal QD size distribution determines the PL FWHM. The growth interruption after the QD formation has been reported to cause coarsening of QDs, leading to a bimodal size distribution.[23] The coarsening is enhanced with increasing the substrate temperature. Since we change the substrate temperature during the growth interruption, the bimodal distribution appears during the growth interruption and is considered to be maintained the feature after capping.

Moreover, we investigated the effect of the capping temperature on the emission intensity of the QDs. Figure 5 shows the integrated PL intensity of the InAs QDs at 20 K as a function of the GaAs capping temperature. Generally, a low temperature growth deteriorates the crystal quality due to defect formation, resulting in a reduction of emission intensity. However, the integrated PL intensity in Fig. 5 increases with decreasing the capping temperature. When

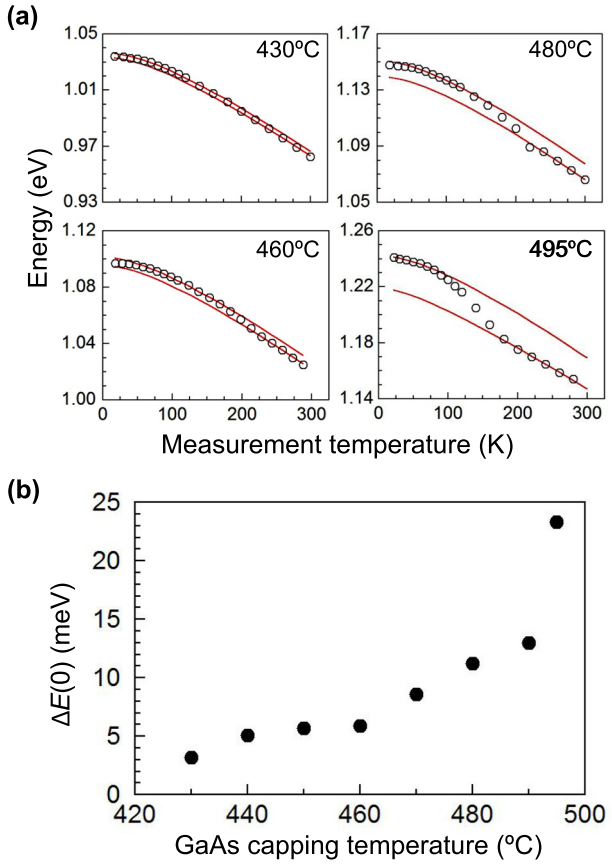

FIG. 4. (a) Measurement temperature dependence of the PL peak energy for various GaAs capping temperatures. The solid lines represent the energy gap shrinkage of the InAs QDs estimated from the Varshni empirical relation. (b) GaAs capping temperature dependence of $\Delta E(0)$, where $\Delta E(0)$ is the energy difference between the energy gaps of the smaller and larger QDs at 0 K.

the capping temperature becomes lower than 460 °C, the intensity starts decreasing again. There are some factors that affect the PL emission intensity: a generation of crystal defects, an increase in oscillator strength, and a decrease in QD density. To clarify whether these factors have an effect, we investigated the recombination lifetime of the QD excitons (τ) by time-resolved PL measurement. Figure 6(a) shows the typical PL decay profiles of the InAs QDs for various capping temperatures, which were recorded at the peak wavelength of the ground-state emission from the QDs. The measurement temperature was 3.4 K. All the profiles can be fitted by a single exponential function. The value of τ

TABLE I. Varshni parameters determined by fitting to the measured data in the low-temperature region below 120 K and the high-temperature region above 220 K.

GaAs capping temperature (°C)	$E(0)$ (eV)	α ($\times 10^{-3}$ eV·K^{-1})	β (K)
430 (low)	1.037	0.374	176
(high)	1.034		
460 (low)	1.101	0.367	149
(high)	1.095		
480 (low)	1.151	0.387	173
(high)	1.140		
495 (low)	1.242	0.378	167
(high)	1.219	0.313	94

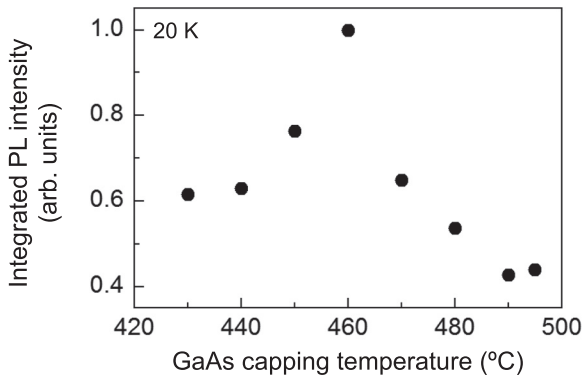

FIG. 5. Integrated PL intensity of the InAs QDs at 20 K as a function of the GaAs capping temperature.

derived from these profiles is plotted as a function of the capping temperature in Fig. 6(b). The recombination lifetime is related to the radiative (τ_r) and non-radiative (τ_{nr}) lifetimes, respectively, by[24]

$$\frac{1}{\tau} = \frac{1}{\tau_r} + \frac{1}{\tau_{nr}}. \quad (2)$$

τ_r is inversely proportional to the oscillator strength given by the electronic dipole transition and the overlap integral of the

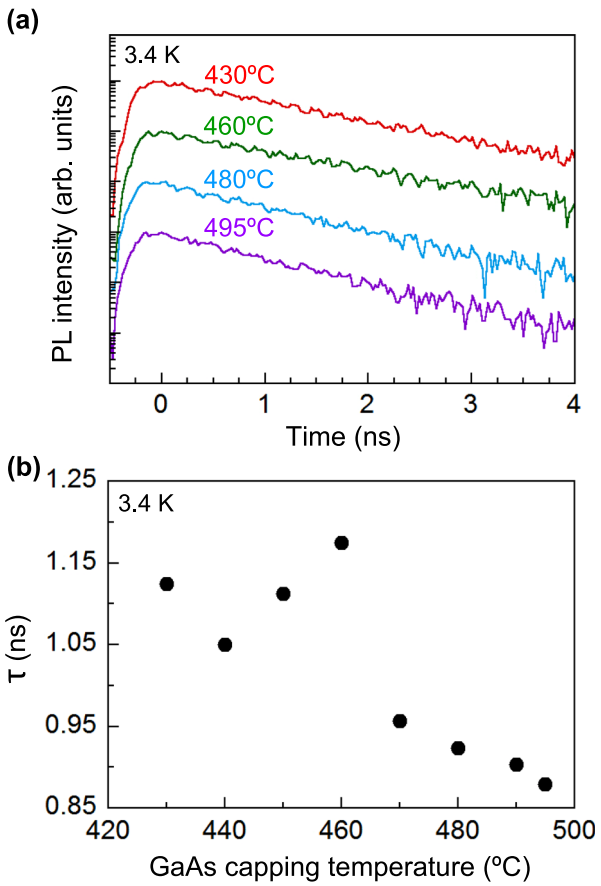

FIG. 6. (a) PL decay profiles of the InAs QDs for various GaAs capping temperatures, which were recorded at the peak wavelength of the ground-state emission from the QDs. (b) GaAs capping temperature dependence of τ, where τ is the recombination lifetime of the InAs QD excitons. The measurement temperature was 3.4 K.

electron and hole wavefunctions.[25] When the QD size, especially the QD height, becomes small at high capping temperatures, the electron wavefunction trends to penetrate deeper into the GaAs cap layer, which leads to a reduction of wavefunction overlap, and therefore, the oscillator strength is reduced.[26,27] Thus, as the capping temperature is lowered, the oscillator strength increases. Therefore, τ_r decreases with decreasing the capping temperature. Conversely, τ_{nr} increases because the relative contribution of carrier trapping at the QD surface defects becomes small for large QDs. When the increment of τ_{nr} exceeds the decrement of τ_r, the measured total lifetime τ increases with increasing the QD size.[27] τ's measured for QDs capped at temperatures higher than 460 °C in Fig. 6(b) exhibits a behavior similar to the results in Ref. 27. On the other hand, we observed that τ decreases for QDs capped below 460 °C. This can be attributed to defect formation induced by low capping temperatures, which leads to a significant reduction of τ_{nr}. The luminescence intensity I is proportional to the quantum yield η given by the ratio of the total measured lifetime to the radiative lifetime: $I \propto \eta = \tau/\tau_r$.[24] τ_r decreases with decreasing the capping temperature, which results in an increase in I. When the capping temperature becomes lower than 460 °C, τ starts decreasing again and I decreases as well. This is consistent with the behavior of the integrated PL intensity shown in Fig. 5.

Next, we discuss the GaAs capping temperature dependence of the linearly polarized PL properties of the InAs QDs. Figure 7 shows the polarized PL intensity ratios of (a) $I_{[001]}/I_{[-110]}$, (b) $I_{[001]}/I_{[110]}$, and (c) $I_{[110]}/I_{[-110]}$ observed from the (110)- and (−110)-cleaved surfaces, and the (001) surface as a function of the capping temperature, where $I_{[001]}$, $I_{[-110]}$, and $I_{[110]}$ denote the ground-state PL intensities polarized along the [001], [−110], and [110] directions, respectively. The measurement temperature was room temperature. The $I_{[001]}/I_{[-110]}$ ratio in Fig. 7(a) is almost constant at capping temperatures higher than 460 °C, while at capping temperatures lower than 460 °C, it increases with decreasing capping temperature. This is explained by the variation in the shape anisotropy of the embedded QDs shown in Fig. 2(c). The PL polarization depends on the confinement direction within the quantum structure because of the selection rules for optical transitions. Since the ground-state PL of QDs with a low aspect ratio is the heavy-hole exciton transition, its polarization is perpendicular to the confinement direction, i.e., the [001] growth direction.[28] Therefore, the polarization component along the [−110] in-plane direction becomes dominant. When the aspect ratio of QDs increases, the vertical confinement is relaxed, and thereby, the heavy- and light-hole states start mixing, which leads to an increase in the [001] polarization component relative to the [−110] component.[29,30] In contrast to the $I_{[001]}/I_{[-110]}$ ratio, the $I_{[001]}/I_{[110]}$ ratio is almost constant at all capping temperatures, as shown in Fig. 7(b). This indicates the constant aspect ratio of the height to the [110] base size of the embedded QDs. In addition, considering the capping temperature dependence of the height of the embedded QDs shown in Fig. 2(b), it is inferred that the [110] base size monotonically increases with decreasing capping temperature and height. This inference is

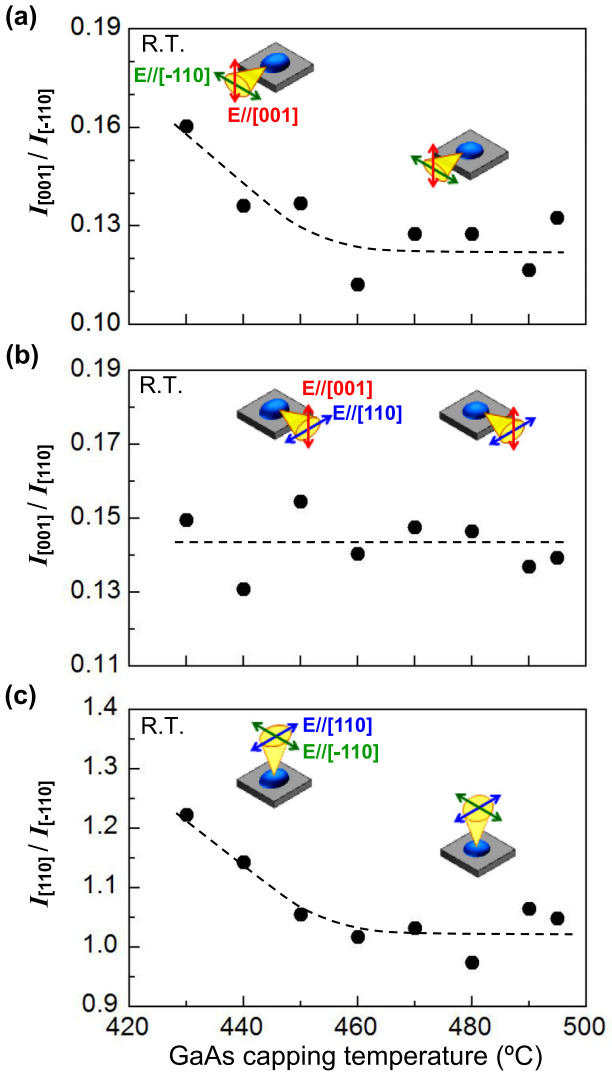

FIG. 7. Polarized PL intensity ratios of (a) $I_{[001]}/I_{[-110]}$, (b) $I_{[001]}/I_{[110]}$, and (c) $I_{[110]}/I_{[-110]}$ observed from the (110)- and (−110)-cleaved surfaces, and the (001) surface as a function of the GaAs capping temperature, where $I_{[001]}$, $I_{[-110]}$, and $I_{[110]}$ denote the ground-state PL intensities polarized along the [001], [−110], and [110] directions, respectively. The measurement temperature was room temperature. The dotted lines are guides to the eyes. The insets are the schematic illustrations of the polarized PL from the InAs QDs with anisotropic shape.

also supported by the data of the in-plane polarization anisotropy in Fig. 7(c). The $I_{[110]}/I_{[-110]}$ ratio, which reflects the in-plane anisotropy of the QD shape, exhibits a behavior similar to that of the $I_{[001]}/I_{[-110]}$ ratio. This indicates that the [110] base size varies similarly with the height. In contrast, the [−110] base size is independent of the capping temperature below 460 °C, as shown in Fig. 2(b). This is considered to be related to the anisotropic growth of the GaAs cap layer on the InAs QDs during the initial capping process rather than the anisotropy of Ga adatom diffusion. Under an As_2 flux, the shape of QDs capped with a thin cap layer has been reported to elongate along the [110] direction at a capping temperature of 420 °C, while it elongated along the opposite [−110] direction at 460 °C.[31] The variation in incorporation rate of Ga adatoms is due to the difference in the atomic steps between the [110] and [−110] directions, which causes the anisotropic growth of the cap layer.[32] Since

the QD morphology greatly varies during the initial capping process, as shown in Fig. 1, the dependence of the size variation on the capping temperature becomes pronounced in the preferential growth direction of the cap layer, which is the [110] direction at low temperatures. Control of the polarization properties is crucial for the development of polarization-insensitive SOAs. We have demonstrated an almost polarization-insensitive optical gain for the cleaved surface of 30-layer stacked InAs/GaAs QDs.[9] The results of this study suggest that a low capping temperature has the potential to achieve polarization insensitivity with fewer stacking layers.

IV. SUMMARY

We investigated the effects of the GaAs capping temperature on the morphological and PL properties of InAs QDs. The QD shrinkage during the capping process was suppressed by decreasing the capping temperature, and thereby, the broadband tuning of the emission wavelength from 1.1 to 1.3 μm was achieved at room temperature. In addition, linearly polarized PL properties that reflected the shape anisotropy of the embedded QDs were observed, in which the [110] polarization component as well as the [001] component increased relative to the [−110] component at capping temperatures lower than 460 °C. These results reveal that not only the emission wavelength but also the polarization anisotropy can be controlled by the capping temperature.

[1]Y. Arakawa and H. Sakaki, Appl. Phys. Lett. **40**, 939 (1982).
[2]D. Bimberg, M. Grundmann, and N. N. Ledentsov, *Quantum Dot Heterostructures* (Wiley, New York, 1998).
[3]H. Shoji, *Semiconductors and Semimetals* (Academic, San Diego, 1999), Vol. 60.
[4]M. Sugawara, N. Hatori, T. Akiyama, Y. Nakata, and H. Ishikawa, Jpn. J. Appl. Phys., Part 2 **40**, L488 (2001).
[5]T. Kita, O. Wada, H. Ebe, Y. Nakata, and M. Sugawara, Jpn. J. Appl. Phys., Part 2 **41**, L1143 (2002).
[6]P. Jayavel, H. Tanaka, T. Kita, O. Wada, H. Ebe, M. Sugawara, J. Tatebayashi, Y. Arakawa, Y. Nakata, and T. Akiyama, Appl. Phys. Lett. **84**, 1820 (2004).
[7]T. Kita, N. Tamura, O. Wada, M. Sugawara, Y. Nakata, H. Ebe, and Y. Arakawa, Appl. Phys. Lett. **88**, 211106 (2006).
[8]T. Inoue, M. Asada, N. Yasuoka, O. Kojima, T. Kita, and O. Wada, Appl. Phys. Lett. **96**, 211906 (2010).
[9]T. Kita, M. Suwa, T. Kaizu, and Y. Harada, J. Appl. Phys. **115**, 233512 (2014).
[10]E. F. Schubert, *Light-Emitting Diodes* (Cambridge University Press, New York, 2003).
[11]Q. Gong, P. Offermans, R. Nötzel, P. M. Koenraad, and J. H. Wolter, Appl. Phys. Lett. **85**, 5697 (2004).
[12]H. Eisele, A. Lenz, R. Heitz, R. Timm, M. Dähne, Y. Temko, T. Suzuki, and K. Jacobi, J. Appl. Phys. **104**, 124301 (2008).
[13]F. Ferdos, S. Wang, Y. Wei, A. Larsson, M. Sadeghi, and Q. Zhao, Appl. Phys. Lett. **81**, 1195 (2002).
[14]K. Nishi, H. Saito, S. Sugou, and J. S. Lee, Appl. Phys. Lett. **74**, 1111 (1999).
[15]N. Ozaki, T. Yasuda, S. Ohkouchi, E. Watanabe, N. Ikeda, Y. Sugimoto, and R. A. Hogg, Jpn. J. Appl. Phys., Part 1 **53**, 04EG10 (2014).
[16]Z. R. Wasilewski, S. Fafard, and J. P. McCaffrey, J. Cryst. Growth **201–202**, 1131 (1999).
[17]Y. Hino, N. Ozaki, S. Ohkouchi, N. Ikeda, and Y. Sugimoto, J. Cryst. Growth **378**, 501 (2013).
[18]C. E. C. Wood, D. Desimone, K. Singer, and G. W. Wicks, J. Appl. Phys. **53**, 4230 (1982).
[19]K. Yamaguchi, Y. Saito, and R. Ohtsubo, Appl. Surf. Sci. **190**, 212 (2002).
[20]Y. P. Varshni, Physica **34**, 149 (1967).
[21]R. Heitz, I. Mukhametzhanov, A. Madhukar, A. Hoffmann, and D. Bimberg, J. Electron. Mater. **28**, 520 (1999).
[22]H. Kissel, U. Müller, C. Walther, W. T. Masselink, Y. I. Mazur, G. G. Tarasov, and M. P. Lisitsa, Phys. Rev. B **62**, 7213 (2000).
[23]T. I. Kamins, G. M. Ribeiro, D. A. A. Ohlberg, and R. S. Williams, J. Appl. Phys. **85**, 1159 (1999).
[24]M. Gurioli, A. Vinattieri, M. Colocci, C. Deparis, J. Massies, G. Neu, A. Bosacchi, and S. Franchi, Phys. Rev. B **44**, 3115 (1991).
[25]U. E. H. Laheld and G. T. Einevoll, Phys. Rev. B **55**, 5184 (1997).
[26]J. Johansen, S. Stobbe, I. S. Nikolaev, T. L. Hansen, P. T. Kristensen, J. M. Hvam, W. L. Vos, and P. Lodahl, Phys. Rev. B **77**, 073303 (2008).
[27]S. Stobbe, J. Johansen, P. T. Kristensen, J. M. Hvam, and P. Lodahl, Phys. Rev. B **80**, 155307 (2009).
[28]E. O. Kane, *Semiconductor and Semimetals* (Academic Press, New York, 1966), Vol. 1.
[29]Y. Ikeuchi, T. Inoue, M. Asada, Y. Harada, T. Kita, E. Taguchi, and H. Yasuda, Appl. Phys. Express **4**, 062001 (2011).
[30]M. Usman, T. Inoue, Y. Harada, G. Klimeck, and T. Kita, Phys. Rev. B **84**, 115321 (2011).
[31]S. Ohkouchi, N. Kumagai, K. Watanabe, S. Iwamoto, and Y. Arakawa, J. Cryst. Growth **378**, 549 (2013).
[32]T. Sugaya, T. Amano, and K. Komori, J. Appl. Phys. **100**, 063107 (2006).